Li et al. Nanoscale Research Letters (2016) 11:271
DOI 10.1186/s11671-016-1486-6

Nanoscale Research Letters

NANO EXPRESS Open Access

Photocatalytic Oxidation of Propylene on Pd-Loaded Anatase TiO_2 Nanotubes Under Visible Light Irradiation

Chen Li[1], Lanlan Zong[1], Qiuye Li[1,2*], Jiwei Zhang[1,2], Jianjun Yang[1,2] and Zhensheng Jin[1]

Abstract

TiO_2 nanotubes attract much attention because of their high photoelectron-chemical and photocatalytic efficiency. But their large band gap leads to a low absorption of the solar light and limits the practical application. How to obtain TiO_2 nanotubes without any dopant and possessing visible light response is a big challenge nowadays. Orthorhombic titanic acid nanotubes (TAN) are a special precursor of TiO_2, which possess large Brunauer-Emmett-Teller (BET) surface areas and strong ion exchange and adsorption capacity. TAN can transform to a novel TiO_2 with a large amount of single-electron-trapped oxygen vacancies (SETOV) during calcination, while their nanotubular structure would be destroyed, and a BET surface area would decrease remarkably. And interestingly, SETOV can lead to a visible light response for this kind of TiO_2. Herein, glucose was penetrated into TAN by the vacuum inhalation method, and TAN would dehydrate to anatase TiO_2, and glucose would undergo thermolysis completely in the calcination process. As a result, the pure TiO_2 nanotubes with visible light response and large BET surface areas were obtained. For further improving the photocatalytic activity, Pd nanoparticles were loaded as the foreign electron traps on TiO_2 nanotubes and the photocatalytic oxidation efficiency of propylene was as high as 71 % under visible light irradiation, and the photostability of the catalyst kept over 90 % after 4 cyclic tests.

Keywords: Anatase TiO_2 nanotubes, Visible light, Titanate nanotubes, Single-electron-trapped oxygen vacancies, Visible light photocatalysis

Background

The last decades have witnessed the flying advance of our society; at the same time, many problems appear. One of the top problems is environmental concern. It has effects on ecological balance, human health, and sustainable development. Photocatalytic elimination of the organic pollutants is one of the efficient ways to alleviate the pollution of the environment and which has been widely studied in the past decades [1–5].

TiO_2 has become the hottest photocatalyst since it was found by Fujishima in 1972 that TiO_2 had the photoelectron-catalytic ability to make water splitting [6]. Since then, a TiO_2 photocatalyst has attracted much attention and has been widely used in degradation of organic pollutants, CO_2 reduction, and so on [7–12]. As is known to all, TiO_2 can be excited by ultraviolet light, which leads to the low utilization of solar light. Besides, its photo-conversion efficiency is very low. To increase the light response region and enhance the efficiency, many approaches have been tried, such as modifying with metal or nonmetal ions [12–16], coupling with other narrow band gap semiconductors [17–19], or sensitizing by various dyes [20–23].

The titanate nanotube is a kind of TiO_2-based material, which possesses a layered structure and a big Brunauer-Emmett-Teller (BET) surface area. The titanate nanotube has many advantages. Firstly, it has a tubular shape with a large surface area, which can provide more adsorption or active sites. Secondly, the layered structure and strong ion exchange ability is

* Correspondence: qiuyeli@henu.edu.cn
[1]National & Local Joint Engineering Research Center for Applied Technology of Hybrid Nanomaterials, Henan University, Kaifeng 475004, People's Republic of China
[2]Collaborative Innovation Center of Nano Functional Materials and Applications of Henan Province, Henan University, Kaifeng 475004, People's Republic of China

favorable for foreign atom doping or incorporating into the crystal lattice. Now, it has been widely used in many fields, such as photocatalysis and solar cells [24, 25]. Our group has systematically studied titanic acid nanotubes (TAN) in the previous work [26–29]. However, it is a pity that TAN itself does not possess photocatalytic activity, until it experiences a high temperature treatment or hydrothermal process, then it turns into a kind of novel TiO_2. The novel TiO_2 has many merits different from the normal TiO_2. Single-electron-trapped oxygen vacancies (SETOV) appeared in the novel TiO_2 when dehydration happens between the layers during the calcination process. SETOV would form a sub-band in the forbidden gap of TiO_2, and as a result, this novel TiO_2 could be excited by visible light [30–32]. However, it also has a natural defect, and the nanotubular structure of TAN will collapse during the dehydration process, resulting in a great decrease of the BET surface area. As well known, the BET surface area of a photocatalyst is very important for its photoactivity.

So how to take full advantage of these excellent merits and avoid the structure collapse of TAN are the key points. In our previous work, we use the "pillar-effect" method, through special measures to put small molecules into TAN, and then they will play a protective role in the tube when calcined. Previously, lanthanum nitrate was selected as a pillar to maintain the tubular morphology [33]. In the process of $La(NO_3)_3$ entering into the TAN, La^{3+} would exchange ions with the wall of the TAN and would incorporate into the crystal lattice of the TAN, so some La^{3+} ions cannot be removed completely. Although the high visible light-responded photocatalytic efficiency on the La-doped TiO_2 nanotubes was achieved, the doped lanthanum would astrict its wide application as a pure anatase TiO_2 precursor. Then we come up with small organic molecules as pillars, hoping to get pure anatase TiO_2 nanotubes. Glucose was selected to substitute $La(NO_3)_3$ to prepare the anatase TiO_2 nanotubes, and the ion exchange process between the incorporated solution and TAN was avoided. In the calcination process, glucose would be removed completely and the pure anatase TiO_2 nanotubes can be obtained. Pd nanoparticles were further loaded as the electron traps on TiO_2 nanotubes to improve the photocatalytic activity. The photo-oxidation removal efficiency of propylene was as high as 71 % under visible light irradiation. These pure anatase TiO_2 nanotubes with a small diameter, large BET surface areas, and visible light response would have a large potential in the field of visible light photocatalysis and solar cell.

Methods

Preparation of the Pure Anatase TiO_2 Nanotubes

The details of the experiments were carried out in accordance with the following steps as simplified in Scheme 1.

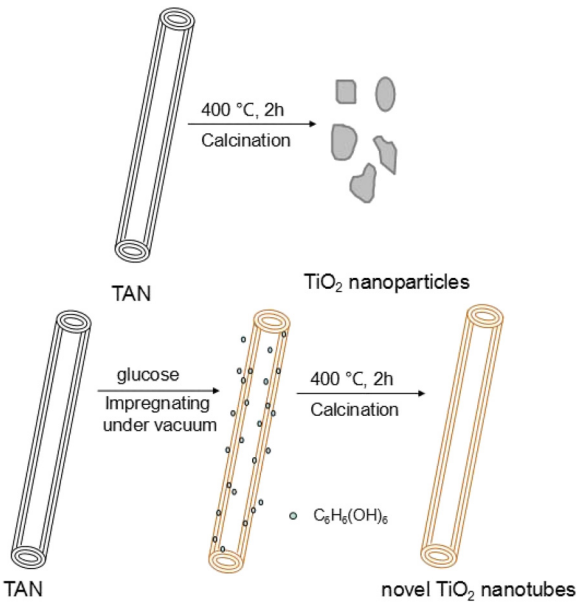

Scheme 1 Formation diagrammatic sketch of TiO_2 nanotubes

Firstly, TAN was prepared by the hydrothermal method reported in our previous work [26]. Then the TAN were soaked with ethanol for 24 h and followed by filtering and drying. After that, TAN was impregnated in 0.01 M glucose solution under vacuum to divert glucose into the nanotube, and then the residual organics of the nanotubes with purified water were cleaned out. At last, the product was calcined in air at 400 °C for 2 h, and as a result, the pure anatase TiO_2 nanotube was obtained. For comparison, the TiO_2 nanoparticles were obtained by calcining the TAN directly at 400 °C for 2 h. To improve the photocatalytic activity, 1 wt.% Pd nanoparticles were loaded as the electron traps on the surface of the TiO_2 nanotubes, which was carried out by the photoreduction of 1 mmol/L $PdCl_2$ in ethanol under UV light for 1 h.

Evaluation of Photocatalytic Activity

The photocatalytic activity was evaluated by monitoring the oxidation of propylene under visible light irradiation. A 300-W Xe arc lamp with a 420-nm cutoff filter was used as the light source ($\lambda \geq 420$ nm, $I = 0.13$ mW cm^{-2}); meanwhile, a water cell was used to prevent the infrared light irradiation. Catalyst powder of 25 mg was spread on the surface of a roughened glass plate (10 cm^2) located in a flat quartz tube reactor. Prior to light irradiation, the system was kept in dark for 2 h until reaching C_3H_6 adsorption-desorption equilibrium. The feed gas (flowing rate was kept at 150 mL h^{-1}) was made up of pure C_3H_6 and Ar, which was stored in a high-pressure cylinder. The content of C_3H_6 was determined at a sensitivity of 1 ppmV by a chromatographic method on line analysis (Shimadzu GC-9A with a flame ionization

detector, a GDX-502 column, and a reactor loaded with a Ni catalyst for the methanization of CO_2); time interval for each analysis is 10 min. The degradation rate of C_3H_6 $(V) = (C_0 - C)/C_0 \times 100$ %, in which C_0 refers to the concentration of feed gas C_3H_6.

Characterization of Samples

A transmission electron microscope (TEM), JEOL JEM-2010, with accelerating voltage of 200 kV, was applied to observe the morphology of the catalysts. The BET specific surface area of the samples was determined by N_2 adsorption-desorption method with a Quadrasorb SI equipment (pretreatment 200 °C/6 h). X-ray diffraction (XRD) patterns were measured on a Philips X'Pert Pro X-ray diffractometer (Holland) (Cu *K*α radiation; 2*θ* range 15° ~ 85°; step size 0.08°; time per step 1.0 s; accelerating voltage 40 kV; applied current 40 mA). Raman shift was recorded with a Raman spectroscopy (RM-1000 Renishaw), with a wavelength range of 100–1750 cm^{-1}. UV-vis diffuse reflectance spectroscopy (DRS) was carried out in diffuse reflection pattern with a spectrophotometer (Lambda 950, Perkin Elmer) equipped with a wavelength range of 200–800 nm ($BaSO_4$ as a reference). Electron spin resonance (ESR) spectra were measured on a Bruker E500 spectrometer at room temperature in ambient air (without supplied vacuum). The catalysts of X-ray photoelectron spectroscopy (XPS) data were obtained through a Kratos AXIS Ultra spectrometer (excitation source: monochromatized Al *K*α (hν = 1486.6 eV); current 10 mA; voltage 15 kV). The binding energies were normalized to the signal for adventitious hydrocarbon at 284.8 eV.

Result and Discussion

Formation Mechanism and Structure of TiO_2 Nanotubes

The TAN can dehydrate to form anatase TiO_2 under calcination. But the one-dimensional nanotubular structure would collapse, and the BET surface areas will decrease remarkably, as shown in Scheme 1. From our previous work, we knew that this kind of TiO_2 possessed a large amount of SETOV that led to a visible light response. How do the nanotubular structure, large BET surface area, and the visible light absorption of this kind of TiO_2 remain? Herein, glucose was selected as the pillar of the nanotube structure, which was soaked into TAN under high vacuum. When calcining a TAN/glucose composite, TAN would dehydrate to anatase TiO_2, and glucose would decompose completely, and as a result, a pure TiO_2 nanotube without any dopant was obtained. The TEM images in Fig. 1 verified this idea of preparation method successfully. Figure 1a shows that the TAN showed a very uniform nanotube morphology and their diameters were ca. 8–10 nm. Figure 1b illustrates that the sample uses glucose as the pillar support and the integrity of the nanotubes implied that glucose was indeed playing the important role of protecting the nanotubular structure. At the same calcination conditions, the tubular shape has partially collapsed and a little part of the short tubes and most nanoparticles left without glucose as the support (as shown in Fig. 1c). Figure 1d illustrates that the layered nanotubular morphology was kept very well after loading the Pd nanoparticles. Palladium existed not only on the surface of the TiO_2 nanotubes but also in the inner of the nanotubes. The average particle sizes of the Pd nanoparticles were ca. 3 nm.

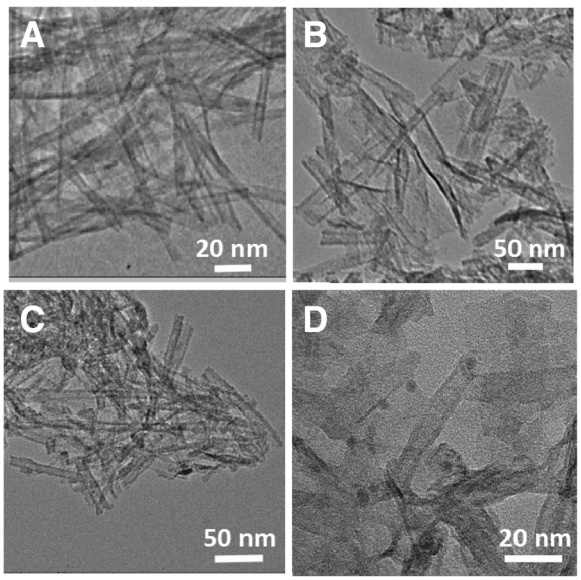

Fig. 1 TEM images of the photocatalysts obtained. **a** TAN. **b** TiO_2 nanotubes. **c** TiO_2 nanoparticles. **d** Pd-loaded TiO_2 nanotubes

Figure 2 shows a typical example of the nitrogen adsorption-desorption isotherms of TiO_2 nanotubes.

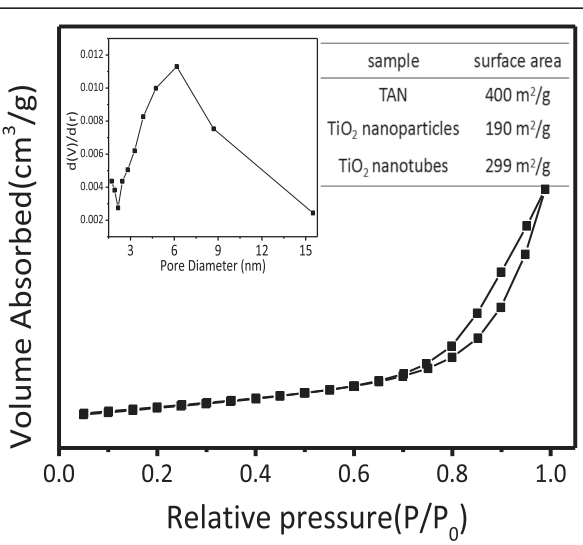

Fig. 2 Nitrogen adsorption-desorption isotherms and pore size distribution curves (*inset*) of as-prepared TiO_2 nanotubes obtained

The sharp decline in the desorption curve and the hysteresis loop at high relative pressure are indicative of mesoporosity. As seen from the inset of Fig. 2, the pore size of TiO_2 was in the range of 4–8 nm. The BET specific surface area of TiO_2 nanotubes was 299 m^2g^{-1}, which increased apparently compared to that of the TiO_2 nanoparticles (S_{BET} = 190 m^2g^{-1}) obtained by calcination of TAN directly in the air at 400 °C. The increased BET surface area should be due to the good nanotubular morphology of TiO_2. The adsorption-desorption isotherm contained an obvious H_2-type hysteresis loop with a highly delayed desorption branch resulted from the hollow structure of the nanotubes, which were in accordance with the HRTEM images of Fig. 1. Furthermore, the BET surface area of the pure TiO_2 nanotubes decreased a little compared with the as-prepared TAN, which should be due to the broken part of the nanotubes.

The phase structure of the photocatalysts was measured by XRD and Raman techniques. The XRD pattern showed that TAN belong to the orthorhombic structure, consistent with the layered titanate (JCPDS No. 47-0124) in the previous reports [29–32]. When calcined at 400 °C, the TAN transformed to anatase TiO_2 completely and the diffraction peaks at about $2\theta = 25.37°$, 37.88°, 48.12°, 53.79°, 55.10°, 62.74°, and 68.79° were assigned to the (101), (004), (200), (105), (211), (204), and (116) crystal faces of anatase, respectively [33]. There is no apparent peak detected belonging to palladium, probably because it had a uniform dispersion and the loading amount was rather low. The Raman spectra shown in Fig. 3b also confirmed the results of XRD, and the TAN has transformed to the pure anatase phase completely. And there is no organic residue on the surface, indicating that glucose had decomposed completely [34].

In our previous researches [28, 29], we found that when TAN were dehydrated at 400 °C or above, a novel anatase TiO_2 containing a large amount of SETOV was obtained. Such a novel TiO_2 contains a high concentration of intrinsic defects in the bulk, but its surface still retains stoichiometric structure. In addition, a high concentration of SETOV is favorable for the formation of a sub-band within the forbidden band of TiO_2. As a result, such a novel TiO_2 can be excited by visible light. In this work, whether the TiO_2 nanotubes prepared from TAN through the pillar effect still possess this kind of SETOV is a question. As can be seen from the ESR spectra in Fig. 4, the present signal at 2.003 is of character peak of SETOV, indicating that the glucose-supported sample contains a certain amount of SETOV, which would help increase the absorption of the visible light region and further be favored to enhance the photocatalytic efficiency.

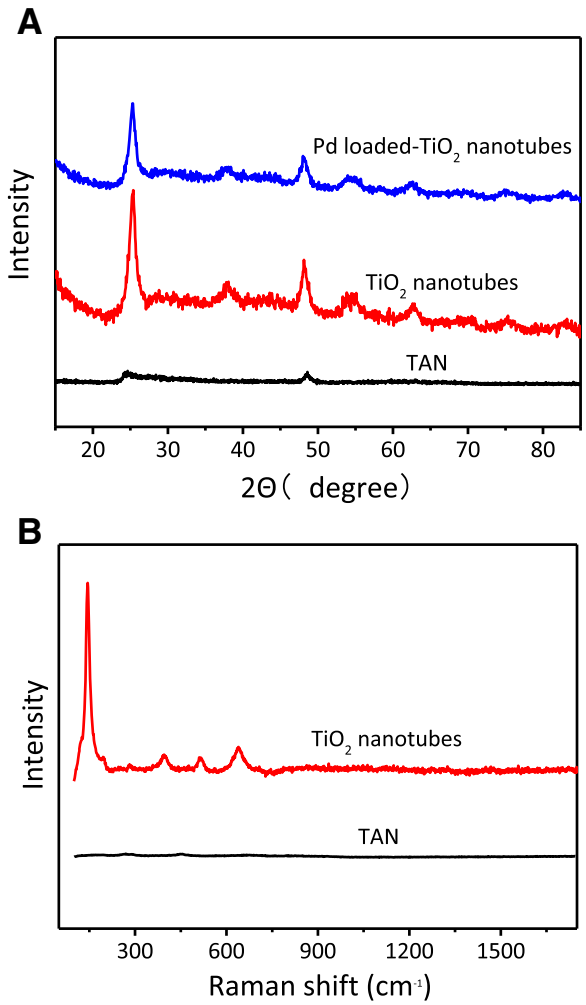

Fig. 3 XRD patterns (**a**) and Raman spectra (**b**) of TAN and Pd-loaded TiO_2 nanotubes obtained

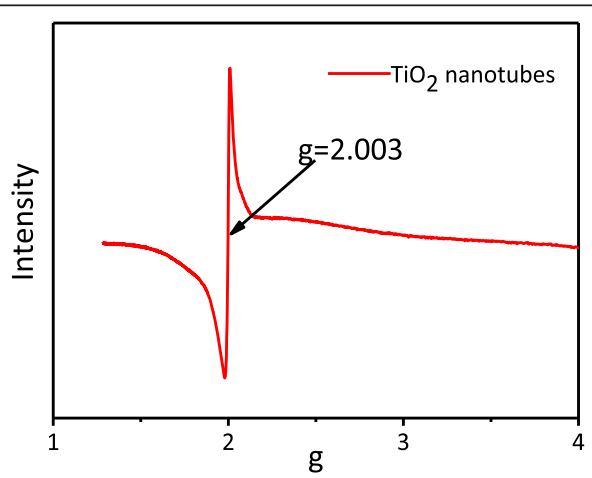

Fig. 4 ESR spectra of TiO_2 nanotubes obtained in ambient air

UV-vis diffuse reflection spectra of the samples were illustrated in Fig. 5. The absorption onset wavelength of TAN is ca. 370 nm, and the energy band gap was calculated to be 3.35 eV. When TAN transformed to TiO_2 nanotubes, the absorption redshifted apparently, which was in accordance with TEM and XRD results. The broad shoulder peak at ca. 400–450 nm in the visible light region should be due to the sub-band formed by SETOV in the band gap of the TiO_2 nanotubes [28]. After loading the Pd nanoparticles on the TiO_2 nanotubes, the visible light absorption enhanced remarkably; this phenomenon should be due to the plasma resonance absorption of the noble metal palladium [35]. This high visible light absorption should be helpful to enhance photocatalytic activity.

The chemical composition and valence state of the surface elements of the Pd-loaded-TiO_2 nanotubes were analyzed by XPS measurement. The chemical states of C1s, Pd 3d, O1s, and Ti 2p species were obtained by analyzing the XPS core levels shown in Fig. 6. The C1s peaks at 284.8 and 288.9 e V were assigned to the contaminative hydrocarbon adsorbed on the sample surface. These results implied that there are no other organic residues remaining on the surface of the catalyst. The binding energies for Pd $3d_{5/2}$ and Pd $3d_{3/2}$ that appeared at 334.8 and 340.0 eV, respectively, explained that the valence state of palladium was Pd^0 [35–38], indicating that the Pd nanoparticles were loaded on the TiO_2 nanotubes successfully. The chemical state of oxygen and titanium are the same with that of the TiO_2 nanoparticles. The peaks at 532.4 and 530.5 eV were corresponding to the crystal lattice oxygen and adsorbed oxygen. Two characteristic peaks of Ti2p that appeared at 458.8 and 464.6 eV in Fig. 6d were indexed to Ti $2p_{1/2}$ and Ti $2p_{3/2}$, respectively, indicating that titanium is entirely at presence of Ti^{4+}.

Electrochemical impedance spectroscopy is helpful to probe the features of surface-modified electrodes. And an EIS spectrum often displays the conductivity of an electrode, and a larger arc radius usually shows a higher charge transfer resistance. So the electron transport properties of the TiO_2 nanoparticles, TiO_2 nanotubes, and 1 % Pd-TiO_2 nanotubes were characterized by EIS and shown in Fig. 7. And the Nyquist plots of the EIS spectra were measured in 0.1 M KOH aqueous solution under visible light irradiation ($\lambda \geq 420$ nm, $I = 0.13$ mW cm^{-2}). The arc radii of the TiO_2 nanoparticles and TiO_2 nanotubes were similar, but they are much larger than that of the 1 % Pd-TiO_2 nanotube electrode. That indicated that the 1 % Pd-TiO_2 nanotubes displayed a much higher separation efficiency of photo-generated electron and hole pairs, which would be beneficial to the improvement of its photocatalytic activity. Therefore, doping the Pd nanoparticles in the TiO_2 nanotubes has a significant impact on the photoelectron conversion efficiency.

Photo-oxidation Removal of Propylene on Pd-Loaded TiO_2 Nanotubes Under Visible Light Irradiation

The photocatalytic activities of the catalysts were evaluated by monitoring oxidation of propylene under visible light irradiation. As can be seen in Fig. 8, the

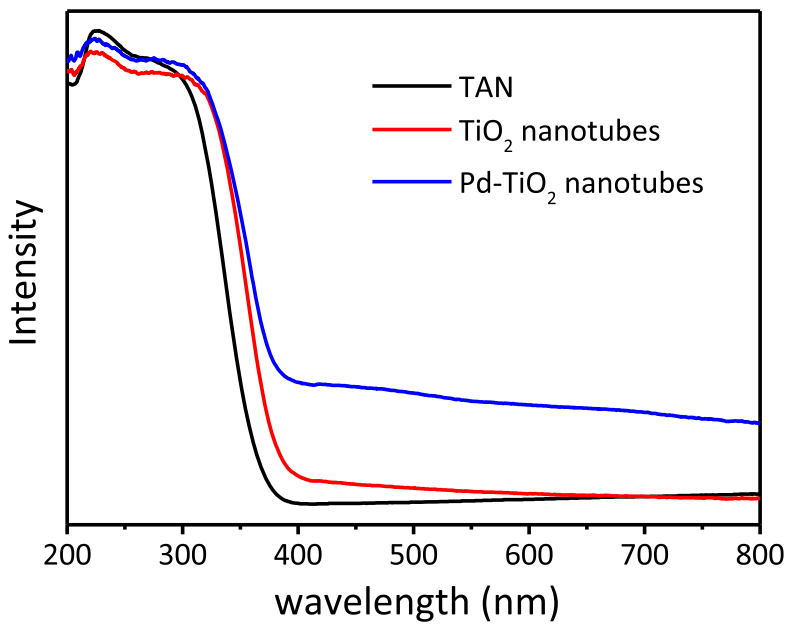

Fig. 5 UV-vis diffuse reflectance spectra of as-prepared TAN, TiO_2 nanotubes, and Pd-loaded TiO_2 nanotubes obtained

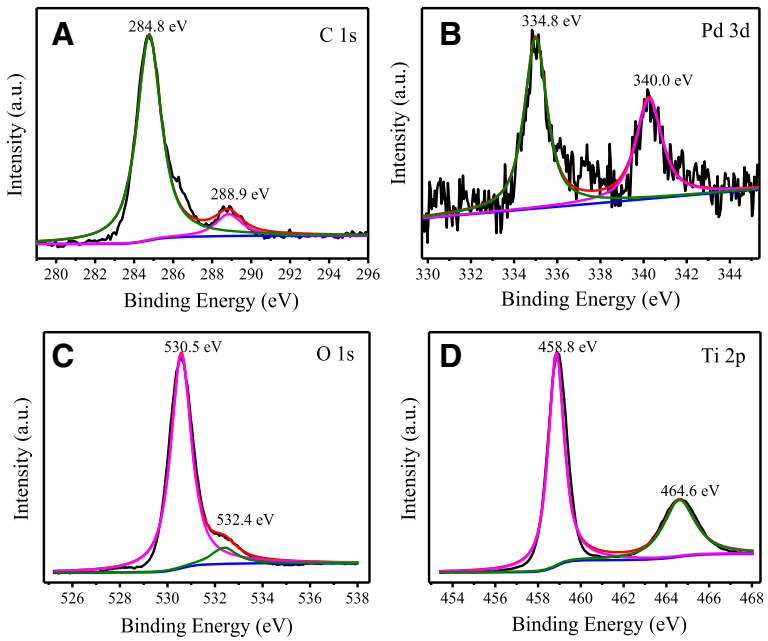

Fig. 6 XPS spectra of Pd-loaded TiO_2 nanotubes obtained: **a** C1s, **b** Pd 3d, **c** O1s, and **d** Ti 2p

degradation yield of C_3H_6 on the TiO_2 nanotubes was 17 %, which was much higher than 11 % of the TiO_2 nanoparticles. The reason should be due to the larger BET surface area and one-dimensional nanotubular morphology of TiO_2 nanotubes. After loading the Pd nanoparticles, the photocatalytic activity increased largely and removal yield of C_3H_6 on the Pd-loaded TiO_2 nanotubes reached 71 %. After loading the Pd nanoparticles, the visible light absorption increased apparently than the bare one, indicating that the utilization efficiency of the incident light increased accordingly. In addition, as a good foreign electron trap, Pd can transfer the photo-generated electrons of the TiO_2 nanotubes, thereby improving the separation efficiency of the charge carriers, so a higher photo-oxidation efficiency of C_3H_6 was obtained. Moreover, comparing with the Pd-loaded La-doped TiO_2 nanotubes in our former work, we found that the photoactivity of the Pd-loaded TiO_2 nanotubes was better than that of the La-doped samples. The reason can be explained as that the La dopant may destroy some lattice of TiO_2 and form a lattice defect, which would become the recombination of the photocharge carriers. From the above analysis, we can conclude that the pure TiO_2 nanotubes with large

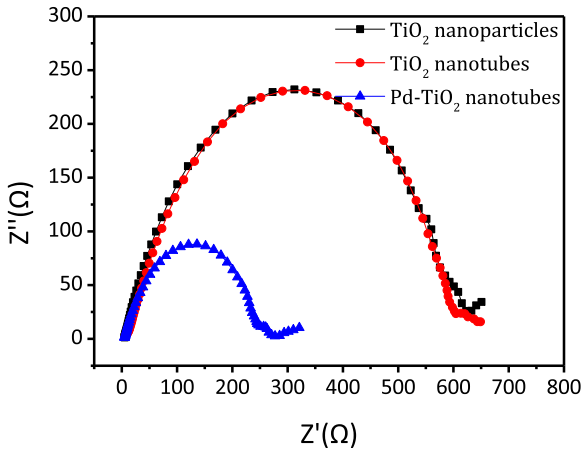

Fig. 7 Electrochemical impedance spectroscopy of TiO_2 nanotubes, TiO_2 nanoparticles, and Pd-loaded TiO_2 nanotubes

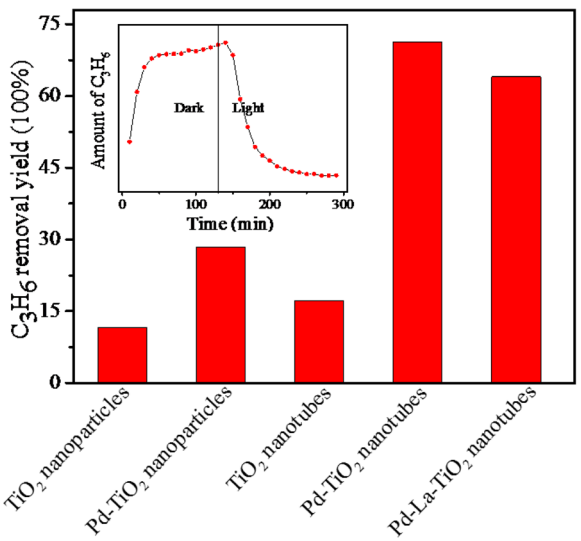

Fig. 8 The yield of photo-oxidation removal of propylene on all samples under visible light

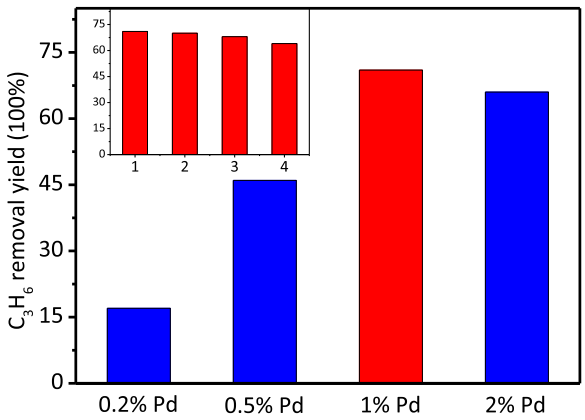

Fig. 9 The yield of photo-oxidation removal of C_3H_6 on different amounts of Pd-loaded TiO_2 nanotubes; photostability test of 1 % Pd-TiO_2 nanotubes displayed in the *inset*

BET surface areas, visible light absorption, and visible light-responded photocatalytic activity have been fabricated from NTA assisted with the pillar effect of glucose.

The effect of loading amount of the Pd nanoparticles on photo-removal efficiency of propylene was investigated in Fig. 9. As can be seen, as the loading amount of Pd increases from 0.2 to 2 %, the removal efficiency of propylene first increased and then decreased. Too little amount of Pd could not trap enough photo-generated electrons to realize the best separation of the charge carriers, while too much amount of Pd would agglomerate and become the recombination centers of the electrons and holes. And as a result, the best photoactivity was obtained as high as 71 % on the sample of the 1 % Pd-loaded TiO_2 nanotubes. Moreover, the photostability of the optimum photocatalysts for propylene removal was evaluated. As shown in the inset of Fig. 9, after four times of circulation experiment, the C_3H_6 removal yield on the 1 % Pd-TiO_2 nanotubes was also kept 64 %, indicating that the photocatalytic efficiency remained over 90 % after a long-term reaction, which testified that the stability of the photocatalyst was excellent.

Conclusions

The pure TiO_2 nanotubes with excellent visible light photoactivity were prepared using TAN as the precursor and glucose as a pillar support. During calcination, TAN would dehydrate into the anatase TiO_2, and glucose went through thermolysis completely. The BET surface area was as large as 299 m^2 g^{-1}, which was much larger than that of the TiO_2 nanoparticles obtained by direct calcination of TAN. The Raman and XPS results proved that there were no organic residues left on the surface or in the phase of the TiO_2 nanotubes. The ESR spectra implied the existence of a large amount of SETOV. When the Pd nanoparticles were loaded on the TiO_2 nanotubes, the photo-oxidation removal efficiency of propylene was as high as 71 % under visible light irradiation, which should be attributed to the higher separation efficiency of the photo-generated electrons and holes, the large BET surface area, and strong visible light absorption of the materials. These pure anatase TiO_2 nanotubes with a small diameter, large BET surface areas, and visible light response would have a large potential in the field of visible light photocatalysis and solar cells.

Acknowledgements

The authors gratefully acknowledge the support of the National Natural Science Foundation of China (Nos. 21103042 and 21471047), Program for Science & Technology Innovation Talents in University of Henan Province (No. 15HASTIT043), and Project of Science and Technology Department of Henan Province of China (Nos. 142102210394, 152102210251).

Authors' contributions

CL carried out the total experiment and wrote the manuscript. LZ and QL participated in the data analysis. QL supervised the project. JY, JZ and ZJ provided the facilities and discussions related to them. All authors read and approved the final manuscript.

Competing interests

The authors declare that they have no competing interests.

Received: 6 March 2016 Accepted: 16 May 2016
Published online: 26 May 2016

References

1. Tian J, Zhao ZH, Kumar A, Boughton RI, Liu H (2014) Recent progress in design, synthesis, and applications of one-dimensional TiO_2 nanostructured surface heterostructures: a review. Chem Soc Rev 43:6920–6937
2. Yu JG, Low JX, Xiao W, Zhou P, Jaroniec M (2014) Enhanced photocatalytic CO_2 reduction activity of anatase TiO_2 by coexposed {001} and {101} facets. J Am Chem Soc 25:8839–8842
3. Tong H, Umezawa N, Ye JH (2011) Visible light photoactivity from a bonding assembly of titanium oxide nanocrystals. Chem Commun 47:4219–4221
4. Cao YH, Li C, Li JL, Li QY, Yang JJ (2015) Magnetically separable Fe_3O_4/AgBr hybrid materials: highly efficient photocatalytic activity and good stability. Nanoscale Res Lett 10:1–6
5. Zhang JF, Zhou P, Liu JJ, Yu JG (2014) New understanding of the difference of photocatalytic activity among anatase, rutile and brookite TiO_2. Phys Chem Chem Phys 16:20382–20386
6. Fujishima A, Honda K (1972) Electrochemical photolysis of water at a semiconductor electrode. Nature 238:37–38
7. Tong XL, Yang P, Wang YW, Qin Y, Guo XY (2014) Enhanced photoelectrochemical water splitting performance of TiO_2 nanotube arrays coated with an ultrathin nitrogen-doped carbon film by molecular layer deposition. Nanoscale 6:6692–6700
8. Cheng XW, Deng XY, Wang P, Liu HL (2015) Coupling TiO_2 nanotubes photoelectrode with Pd nano-particles and reduced graphene oxide for enhanced photocatalytic decomposition of diclofenac and mechanism insights. Sep Purif Technol 154:51–59
9. Lv J, Gao HZ, Wang HG, Lu XJ, Xu GQ, Wang DM, Chen Z, Zhang XY, Zheng ZX, Wu YC (2015) Controlled deposition and enhanced visible light photocatalytic performance of Pt-modified TiO_2 nanotube arrays. Appl Surf Sci 351:225–231
10. Li X, Liu HL, Luo DL, Li JT, Huang Y, Li HL, Fang YP, Xu YH, Zhu L (2012) Adsorption of CO_2 on heterostructure CdS(Bi_2S_3)/TiO_2 nanotube photocatalysts and their photocatalytic activities in the reduction of CO_2 to methanol under visible light irradiation. Chem Eng J 180:151–158
11. Wang J, Yang PJ, Cao BY, Zhao JH, Zhu ZP (2015) Photocatalytic carbon–carbon bond formation with concurrent hydrogen evolution on the Pt/TiO_2 nanotube. Appl Surf Sci 325:86–90
12. Zhang YJ, Zhao GH, Shi HJ, Zhang YN, Huang WN, Huang XF, Wu ZY (2015) Photoelectrocatalytic glucose oxidation to promote hydrogen production over periodically ordered TiO_2 nanotube arrays assembled of Pd quantum dots. Electrochim Acta 174:93–101

13. Liu JW, Han R, Zhao Y, Wang HT, Lu WJ, Yu TF, Zhang YX (2011) Enhanced photoactivity of V-N codoped TiO_2 derived from a two-step hydrothermal procedure for the degradation of PCP-Na under visible light irradiation. J Phys Chem C 115:4507–4515
14. Xing LB, Yang JL, Yu Y (2012) Ti^{3+} in the surface of titanium dioxide: generation, properties and photocatalytic application. J Nanomater 8315:24–37
15. Wang Y, Feng CX, Zhang M, Yang JJ, Zhang ZJ (2010) Enhanced visible light photocatalytic activity of N-doped TiO_2 in relation to single-electron-trapped oxygen vacancy and doped-nitrogen. Appl Catal B 100:84–90
16. Ren FZ, Li HY, Wang YX, Yang JJ (2015) Enhanced photocatalytic oxidation of propylene over V-doped TiO_2 photocatalyst: reaction mechanism between V^{5+} and single-electron-trapped oxygen vacancy. Appl Catal B 176:160–172
17. Li HY, Ren FZ, Liu JF, Wang QL, Li QY, Yang JJ, Wang YX (2015) Endowing single-electron-trapped oxygen vacancy self-modified titanium dioxide with visible-light photocatalytic activity by grafting Fe(III) nanocluster. Appl Catal B 172:37–45
18. Zhang Y, Lu JN, Hoffmann MR, Wang Q, Cong YQ, Wang Q, Jin H (2015) Synthesis of g-C_3N_4/Bi_2O_3/TiO_2 composite nanotubes: enhanced activity under visible light irradiation and improved photoelectrochemical activity. RSC Adv 5:48983–48991
19. Min SX, Lu GX (2012) Sites for High efficient photocatalytic hydrogen evolution on a limited-layered MoS_2 cocatalyst confined on graphene sheets-the role of graphene. J Phys Chem C 116:25415–25424
20. Xiang QJ, Yu JG, Jaroniec M (2012) Synergetic effect of MoS_2 and graphene as cocatalysts for enhanced photocatalytic H_2 production activity of TiO_2 nanoparticles. J Am Chem Soc 134:6575–6578
21. Meen TH, Tsai JK, Tu YS, Wu TC, Hsu WD, Chang SJ (2014) Optimization of the dye-sensitized solar cell performance by mechanical compression. Nanoscale Res Lett 9:1–8
22. Guo ZC, Chen B, Mu JB, Zhang MY, Zhang P, Zhang ZY, Wang JF, Zhang X, Sun YY, Shao CL, Liu YC (2012) Ronphthalocyanine/TiO_2 nanofiber heterostructures with enhanced visible photocatalytic activity assisted with H_2O_2. J Hazard Mater 219–220:156–163
23. Mele G, Annese C, Accolti LD, Riccardis AD, Fusco C, Palmisano L, Scarlino A, Vasapollo G (2015) Photoreduction of carbon dioxide to formic acid in aqueous suspension: a comparison between phthalocyanine/TiO_2 and porphyrin/TiO_2 catalysed processes. Molecules 20:396–415
24. Altın İ, Sökmen M, Bıyıklıoğlu Z (2015) Quaternized zinc (II) phthalocyanine-sensitized TiO2: surfactant-modified sol-gel synthesis, characterization and photocatalytic applications. Desalin Water Treat 640:1–12
25. Liu YX, Wang ZL, Wang WD, Huang WX (2014) Engineering highly active TiO_2 photocatalysts via the surface-phase junction strategy employing a titanate nanotube precursor. J Catal 310:16–23
26. Wang XY, Sun LD, Zhang S, Wang X (2014) Small-diameter TiO_2 nanotubes achieved by an optimized two-step anodization for efficient dye-sensitized solar cells. ACS Appl Mater Interfaces 6:1361–1365
27. Yang JJ, Jin ZS, Wang XD, Li W, Zhang JW, Zhang SL, Guo XY, Zhang ZJ (2003) Study on composition, structure and formation process of nanotube $Na_2Ti_2O_4(OH)_2$. Dalton Trans 20:3898–3901
28. Zhang JW, Guo XY, Jin ZS, Zhang SL, Zhou JF, Zhang ZJ (2003) TEM study on the formation process of TiO_2 nanotubes. Chinese Chem Lett 14:419–422
29. Zhang M, Jin ZS, Zhang JW, Guo XY, Yang JJ, Li W, Wang XD, Zhang ZJ (2004) Effect of annealing temperature on morphology, structure and photocatalytic behavior of nanotubed $H_2Ti_2O_4(OH)_2$. J Mol Catal A-Chem 217:203–210
30. Zhang SL, Li W, Jin ZS, Yang JJ, Zhang JW, Du ZL, Zhang ZJ (2004) Study on ESR and inter-related properties of vacuum-dehydrated nanotubed titanic acid. J Solid State Chem 177:1365–1371
31. Li W, Jin ZS, Yang JJ, Zhang ZJ (2003) Influence of vacuum dehydration and visible light irradiation on ESR property of nanotube titanic acid. Photo Graphic Sci Photochem 21:273–279
32. Zhang JW, Jin ZS, Feng CX, Yu LG, Zhang JW, Zhang ZJ (2011) ESR study on the visible photocatalytic mechanism of nitrogen-doped novel TiO_2 synergistic effect of two kinds of oxygen vacancies. J Solid State Chem 184:3066–3073
33. Zong LL, Li QY, Zhang JW, Wang XD, Yang JJ (2013) Preparation of Pd-loaded La-doped TiO_2 nanotubes and investigation of their photocatalytic activity under visible light. J Nanopart Res 15:2042–2050
34. Yang HG, Sun CH, Qiao SZ (2008) Anatase TiO_2 single crystals with a large percentage of reactive facets. Nature 453:638–641
35. Huo JC, Hu YJ, Jiang H, Li CZ (2014) In situ surface hydrogenation synthesis of Ti^{3+} self-doped TiO_2 with enhanced visible light photoactivity. Nanoscale 6:9078–9084
36. Zhong JB, Lu Y, Jiang WD, Meng QM, He XY, Li JZ, Chen YQ (2009) Characterization and photocatalytic property of Pd/TiO_2 with the oxidation of gaseous benzene. J Hazard Mater 168:1632–1635
37. Zhou WJ, Guan Y, Wang DZ, Zhang XH, Liu D, Jiang HD, Wang JY, Liu XG, Liu H, Chen SW (2014) PdO/TiO_2 and Pd/TiO_2 heterostructured nanobelts with enhanced photocatalytic activity. Chem Asian J 9:1648–1654
38. Wu ZB, Sheng ZY, Liu Y, Wang HQ, Tang N, Wang J (2009) Characterization and activity of Pd-modified TiO_2 catalysts for photocatalytic oxidation of NO in gas phase. J Hazard Mater 164:542–548